Interactions of cytidine with N^2-functionalized guanosines and cytidine–cytidine exchange involving a GC pair — NMR and fluorescence spectroscopic study

Sanela Martic, Gang Wu, and Suning Wang

Abstract: Two N^2-functionalized guanosines by diphenylaminobiphenyl and di(2-pyridyl)aminobiphenyl have been found to act as the effective probes for G–C interactions in organic media. Because of the highly emissive nature of the N^2-functionalized guanosines in the visible region, the GC base pair formation event accompanied by distinct fluorescence quenching can be readily monitored by fluorescence spectroscopy. NMR and fluorescence results confirm that the N^2-arylguanosines form H-bonded pairs with cytidine, selectively. An unusual exchange pathway between non-bound cytidine and bound cytidine, in the GC pair, has been identified and extensively studied by NMR methods.

Key words: N^2-guanosine, GC pair and cytidine exchange, fluorescence, NMR, hydrogen bonding.

Résumé : On a trouvé que deux guanosines fonctionnalisées en N^2 par des groupes diphénylaminobiphényle et di(2-pyridyl)aminophényle peuvent agir comme sondes efficaces pour les interactions G–C dans des milieux organiques. En raison du grand pouvoir émetteur des guanosines fonctionnalisées en N^2 dans la région visible, il est très facile par le biais de la spectroscopie de fluorescence de détecter la fluorescence distincte de piégeage qui accompagne la formation d'une paire de base GC. Les résultats de la RMN et de la fluorescence confirment que les N^2-arylguanosines forment sélectivement des paires avec la cytidine, par le biais de liaisons hydrogènes. Faisant appel à des études par RMN, on a identifié et étudié une voie d'échange inhabituelle entre la cytidine non liée et la cytidine liée, dans la paire GC.

Mots-clés : N^2-guanosine, paire GC, échange de cytidine, fluorescence, RMN, liaison hydrogène.

[Traduit par la Rédaction]

Introduction

Among the nucleobases, guanine displays the most versatile H-bonding patterns, including Hoogsteen or Watson–Crick interactions, or combination thereof, and is thus a valuable building block in supramolecular chemistry.[1] In addition, the hydrogen-bonding motifs of guanine, such as G-quartets, are also known to have important and unique biological functions.[2] Hence, developing new functionalized guanosines to facilitate the study of various H-bonding patterns and self-assembled structures involving guanine has been a very active research area. We have shown recently that the attachment of an aryl group, such as a non-emissive *n*-butylphenyl group, at the N^2 site of the guanosine does not disrupt the formation of G-quartet and G-octamer via H-bonds in the presence of alkaline or alkaline-earth metal ions.[3] Building on this knowledge, we have reported recently a class of new luminescent hydrophilic N^2-arylguanosines including **G1** and **G2** shown in Chart 1.[4] Because of the highly emissive nature of the N^2-functionalized guanosines and their strong absorptions in the visible spectra, we have shown that they can be used effectively in studying interactions of guanosines with metal ions such as Zn(II) via a combination of fluorescence, CD, and NMR spectroscopic methods.[4] In addition, the complementary base for guanine in Watson–Crick interactions is cytosine; hence, various functionalized guanosines or cytidines have been used previously to study the formation of the GC base pair and the charge-transfer phenomenon via the GC pair between fluorescent donor and acceptor.[5] To our best knowledge, however, there have been no reports on GC base pairs involving fluorescent N^2-functionalized guanosines.[6] To examine the impact of N^2-functionalization of guanosine on GC pair formation, we investigated the interactions of the native cytidine with **G1** and **G2** by both NMR and fluorescent spectroscopic methods. However, because **G1** and **G2** have poor solubilities in organic solvents and are sparingly soluble in water or the mixture of water and alcohols, which also compete for H bonds with guanosine and cytidine leading to complex H-bond patterns, no meaningful data could be obtained. To overcome this problem, we converted **G1** and **G2** to lipophilic guanosines by protecting OH moieties with acetyl groups, which greatly improved their solubility. The resulting **G1A** and **G2A** guanosines display selective H-bonding with cytidine in solvents such as CH_2Cl_2 that

Received 3 December 2009. Accepted 28 February 2010. Published on the NRC Research Press Web site at canjchem.nrc.ca on 5 May 2010.

S. Martic, G. Wu, and S. Wang.[1] Department of Chemistry, Queen's University, Kingston, ON K7L 3N6, Canada.

[1]Corresponding author (e-mail: wangs@chem.queensu.ca).

Chart 1.

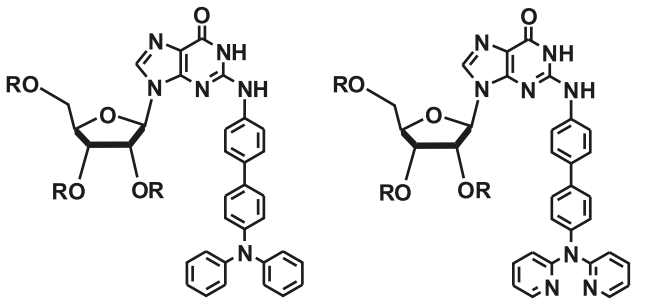

can be monitored by both NMR and fluorescent spectra. The key results are reported herein.

Experimental section

All reagents were purchased from Aldrich Chemical Co. and used without further purification unless stated otherwise. Acetic anhydride, triethylamine, and acetonitrile were freshly distilled under N_2 prior to acetylation reactions. Low-resolution and high-resolution mass spectrometry experiments were performed using the electrospray ionization mode on QSTAR XL MS/MS Systems using Analyst QS Method. Excitation and emission spectra were recorded on a Photon Technologies International QuantaMaster Model C-60 spectrometer. Molecular orbital and molecular geometry calculations were performed using Gaussian 03 program suite. Calculations were carried out at the B3LYP level of theory using 6–31G** as the basis set for all atoms.

Fluorescence experiments

Excitation and emission spectra were recorded on a Photon Technologies International QuantaMaster Model C-60 spectrometer. To the prepared solutions of **G1A** (2.5×10^{-5} mol/L) and **G2A** (2.5×10^{-5} mol/L) in CH_2Cl_2, the solution of **4-C** (6.0×10^{-3} mol/L) was added in 5 μL aliquots.

NMR experiments

All 1D and 2D NMR experiments were recorded on Bruker Avance 400 MHz or 600 MHz spectrometer at 298 K, unless otherwise specified. ^{1}H NMR titrations were performed using the solutions of **G1A** (6.8×10^{-4} mol/L) or **G2A** (1.6×10^{-2} mol/L) in CD_2Cl_2 with the solution of **4-C** in CD_2Cl_2 being added in 10 μL aliquots. DOSY NMR experiments were carried out with Bruker Avance-600 MHz spectrometer using the pulse sequence of longitudinal eddy current delay (LED) with bipolar-gradient pulses. The diffusion period was varied from 50 to 90 ms. Calibration of the field gradient strength was achieved by measuring the value of translational diffusion coefficient (D_t) for the residual ^{1}H signal in D_2O, $D_t = 1.91 \times 10^{-9}$ m^2/s. All NOESY spectra at 298 K were acquired using a mixing time of 0.3 or 0.4 s and the 10 s recycling delay. Phase-sensitive NOESY experiment at 195 K was performed using a mixing time of 0.1 s and a 2 s recycling delay. Phase-sensitive ROESY NMR spectra were recorded on 400 MHz spectrometer at 195 K using a variable mixing times of 0.08, 0.1, and 0.3 s and the 3 s relaxation delay.

Synthesis of 2′,3′,5′-*O*-triacetyl-N^2-(*p*-4,4′-biphenyldiphenylamino)guanosine (G1A)

To a suspension of N^2-(*p*-4,4′-biphenyldiphenylamino)-guanosine, **G1**, (0.34 g, 0.57 mmol) and dimethylaminopyridine (0.005 g, 0.04 mmol) in dry acetonitrile (10 mL), freshly distilled triethylamine (0.30 mL, 2.21 mmol) was added. After stirring for 5 min, freshly distilled acetic anhydride (0.19 mL, 2.00 mmol) was added dropwise over 5 min, and the mixture was stirred for 2 h at room temperature. The reaction mixture was quenched with methanol (5 mL), and the organic solvents were removed to dryness. The residue was treated using the chromatographic column on CH_2Cl_2 and CH_2Cl_2/MeOH (95:5, *v*/*v*) as the eluents to give **G1A** as the white solid. Yield: 0.17 g (43%). Mp > 300 °C. UV absorption λ_{max} (CH_2Cl_2), nm (ε dm^{3}mol^{-1}cm^{-1}): 236 (24 040) and 343 (36 272). Fluorescence (CH_2Cl_2): λ_{ex} = 362 nm and λ_{em} = 410 nm. ^{1}H NMR (400 MHz, DMSO-d_6, 298 K) δ (ppm): 10.82 (1H, br s, N_1H), 8.96 (1H, br s, N_2H), 8.00 (1H, s), 7.61–7.58 (6H, m, *J* = 5.8, 8.6 Hz, Ph), 7.32 (4H, t, *J* = 7.9 Hz, Ph), 7.05 (8H, m, *J* = 7.8, 8.5 Hz, Ph), 6.02 (1H, d, *J* = 5.0 Hz, 1′-H), 6.00 (1H, t, *J* = 5.8 Hz, 2′-H), 5.37 (1H, t, *J* = 5.7 Hz, 3′-H), 4.28 (1H, dd, *J* = 4.4, 5.3 Hz, 4′-H), 4.20 (1H, m, *J* = 4.1, 12.1 Hz, 5′-H), 4.13 (1H, m, *J* = 4.1, 12.4 Hz, 5′-H), 2.07 (3H, s, CH_3), 2.05 (3H, s, CH_3), 1.84 (3H, s, CH_3). ^{13}C NMR (500 MHz, MeOD) δ (ppm): 171.2, 170.1, 169.9, 148.1, 138.1, 134.3, 129.6 (6C), 127.6 (2C), 127.1 (2C), 124.6 (6C), 124.1 (2C), 123.3 (2C), 122.3 (2C), 121.1, 115.6, 96.8 (2C), 87.5 ($C_{1'}$), 80.1 ($C_{4'}$), 72.6 ($C_{2'}$), 70.9 ($C_{3'}$), 63.1 ($C_{5'}$), 19.6 (CH_3), 19.5 (CH_3), 19.4 (CH_3). ESI-MS$^+$ *m*/*z*: 729.2465 [M + H]$^+$. HRMS-EI$^+$ *m*/*z* calcd. for $C_{40}H_{36}N_6O_8$: 728.2594, found: 728.2538.

Synthesis of 2′,3′,5′-*O*-triacetyl-N^2-(*p*-4,4′-biphenyldipyridylamino)guanosine (G2A)

G2A was obtained using the same procedure as for **G1A** with **G2** as the starting material. Yield: 0.08 g (40%). Mp 241–250 °C. UV absorption λ_{max} (CH_2Cl_2), nm (ε dm^{3}mol^{-1}cm^{-1}): 235 (24 003) and 319 (50 240). Fluorescence (CH_2Cl_2): λ_{ex} = 344 nm and λ_{em} = 386 nm. ^{1}H NMR (400 MHz, DMSO-d_6, 298 K) δ (ppm): 10.83 (1H, br s, N_1H), 8.97 (1H, br s, N_2H), 8.25 (2H, d, *J* = 3.7 Hz, Py), 8.02 (1H, s, 8-H), 7.72–7.65 (8H, m, *J* = 7.8, 8.4 Hz, Ph), 7.16 (2H, d, *J* = 8.4 Hz, Ph), 7.04 (2H, d, *J* = 5.3 Hz, Py), 6.99 (2H, d, *J* = 8.8 Hz, Py), 6.08 (1H, d, *J* = 5.3 Hz, 1′-H), 6.01 (1H, t, *J* = 5.8 Hz, 2′-H), 5.39 (1H, t, *J* = 5.7 Hz, 3′-H), 4.28 (1H, m, *J* = 4.3, 9.6 Hz, 4′-H), 4.22 (1H, m, *J* = 3.9, 12.4 Hz, 5′-H), 4.19 (1H, m, *J* = 3.9, 12.3 Hz, 5′-H), 2.09 (3H, s, CH_3), 2.06 (3H, s, CH_3), 1.85 (3H, s, CH_3). ^{13}C NMR (500 MHz, MeOD) δ (ppm): 170.9, 170.2, 170.1, 158.2, 150.4, 147.9 (3C), 144.1, 138.8 (3C), 138.4, 138.1, 137.6, 136.4, 127.9 (3C), 127.3 (2C), 127.2 (3C), 122.5 (2C), 119.0 (2C), 117.9 (2C), 87.6 ($C_{1'}$), 80.0 ($C_{4'}$), 72.5 ($C_{2'}$), 70.8 ($C_{3'}$), 62.8 ($C_{5'}$), 19.3 (CH_3), 19.2 (CH_3), 19.1 (CH_3). ESI-MS$^+$ *m*/*z*: 731.8851 [M + H]$^+$. HRMS-ESI$^+$ *m*/*z* calcd. for $C_{38}H_{34}N_8O_8$ + H: 731.2572, found: 731.2578.

Synthesis of 2′,3′,5′-*O*,N^2-tetraacetyl-N^2-(*p*-4,4′-biphenyldipyridylamino)guanosine (G2B)

G2B was isolated as a side product from the same reaction for **G2A**. Yield: 0.03 g (18%). Mp 156–164 °C. ^{1}H NMR (400 MHz, CD_3CN, 298 K) δ (ppm): 12.98 (broad, N_1H, 1H), 8.24 (d, J = 4.5 Hz, 2H), 7.82 (d, J = 8.4 Hz, 2H), 7.73 (s, 1H, H_8), 7.72 (d, J = 6.5 Hz, 2H), 7.65 (dt, J = 1.8, 9.1 Hz, 2H), 7.48 (d, J = 8.4 Hz, 2H), 7.21 (d, J = 8.5 Hz, 2H), 7.02 (m, 4H), 5.75 (d, J = 4.6 Hz, 1H, $H_{1'}$), 5.57 (t, J = 4.9 Hz, 1H, $H_{2'}$), 4.41 (t, J = 6.0 Hz, 1H, $H_{3'}$), 4.05 (m, J = 5.1, 11.5 Hz, 1H, $H_{4'}$), 3.71 (m, 2H, $H_{5'}$, $H_{5''}$), 2.03 (s, CH_3, 3H), 1.94 (s, CH_3, 3H), 1.88 (s, CH_3, 3H), 1.86 (s, CH_3, 3H). ^{13}C NMR (400 MHz, CD_3CN, 298 K) δ (ppm): 175.7, 170.2, 169.4, 169.3, 158.1 (2C), 155.3, 150.5, 148.3, 147.5 (2C), 145.4, 140.7, 139.4, 138.0 (2C), 137.7 (2C), 135.9, 129.7 (2C), 128.4 (2C), 127.9 (2C), 127.3 (2C), 121.9, 118.6 (2C), 117.3, 87.9 (C_1), 79.4 (C_4), 71.9 (C_2), 70.7 (C_3), 63.8 (C_5), 25.8 (CH_3), 19.8 (CH_3), 19.6 (CH_3), 19.5 (CH_3). HRMS-ESI$^+$ m/z calcd. for $C_{40}H_{36}N_8O_9{\cdot}H^+$: 773.2678, found: 773.2666.

Results and discussion

NMR measurements

GC base pair formation

The structure of the cytidine (**4-C**) used in the study and the GC base pair with labels are shown in Chart 2. ^{1}H NMR spectra indicated that in the absence of **4-C**, **G1A** and **G2A** exist predominantly as monomers in CD_2Cl_2 at 298 K. The addition of **4-C** to the solution of **G1A** or **G2A** in CD_2Cl_2 results in upfield shifts of the imino and amino resonances of the guanine and cytosine units, indicative of H-bonding. As shown in Fig. 1, upon [**G1A**]:[**4-C**] base pair formation, a slight change was observed for the phenyl protons (H_o) directly attached to the N^2-site of guanine, while the H_8 signal of the guanine ring remains virtually unchanged. The most significant change is observed for the H_6 and H_5 resonances of **4-C**, which shift ~ 0.1–0.3 ppm upfield. Upon cooling to 228 K, the [**G1A**]:[**4-C**] dimer can be clearly identified through the sharp peaks at ~ 13.1, 12.2, and 10.7 ppm that can be assigned to the N_1H (**G1A**), N_4H (**4-C**), and N_2H (**G1A**), respectively, as presented in Fig. 2. At 228 K, the NOE cross peaks are of the same phase as the diagonal peaks. The key NOE cross peaks between the N_1H (**G1A**) with N_4H (**4-C**) in the GC base pair were observed in the NOESY NMR spectrum, confirming the GC pair formation. The GC pair formation was further supported by ESI-MS data, with a peak at m/z 1140 identified as [**G1A**:**4-C** + H]$^+$ (see Fig. S1 in the Supplementary data). Similar NMR and ESI-MS data were also obtained for the [**G2A**]:[**4-C**] base pair (see Figs. S2–S4 in the Supplementary data). The relative ribose stereogeometry of the GC base pair was assigned by NOESY NMR and was found to be syn for both N^2-arylguanosines, owing to the strong NOE cross peak between its H_1 and H_8, and anti for **4-C**, judging from the strong NOE between its H_2 and H_6 protons.[7] An association constant could not be determined by NMR dilution method because of the strong GC association. As a control study, we also examined the interaction of 2′,3′,5′-*O*,N^2-tetraacetyl-N^2-(*p*-4,4′-biphenyldipyridylamino)guanosine (**G2B**) with **4-C**, where the H-donor site of the N^2 group is blocked by an acetyl group. Not surprisingly, **G2B** did not form a GC dimer as confirmed by NMR (see Fig. S5 in the Supplementary data for NMR). Thus, the NMR data established unequivocally that the N^2-functionalization by an aryl group does not impede the ability of the guanosine to form a H-bonded base pair with cytidine.

Chart 2.

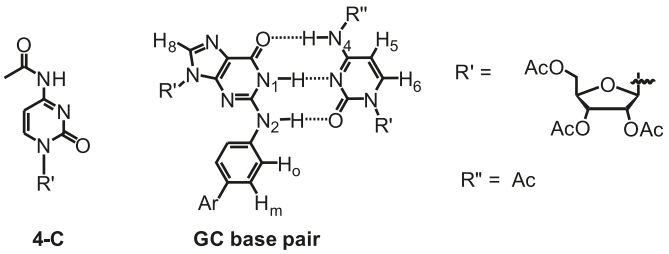

Dynamic exchange of non-bound and bound 4-C in the GC pair

Although the GC base pair formation has been extensively investigated, little is known about the interaction and the exchange mechanism of a GC pair with non-bound G or C. A previous NMR study on the interaction of a GC pair with free guanosine has identified a GCG trimer.[8] However, the exact nature of the interactions between the GC pair and free cytidine remains unclear. The GC pair formed by **G1A** and **G2A** with **4-C** provided us an opportunity to study such interactions by NMR methods. As shown in Fig. 3, the addition of more than 1 equiv. of **4-C** to the solution of **G1A** results in the sharpening of the N^1H and N_2H (**G1A**) resonances along with a slight downfield shift. Surprisingly, the N_4H (**4-C**) proton is shifted upfield (~3 ppm) and broadened, indicating a dynamic process. The overall chemical shift positions and the sharpness of the exchangeable **G1A** protons indicate the complex formation by H-bonds. At [**G1A**]:[**4-C**] $\simeq$ 1:4 ratio, the chemical shifts of the **G1A** protons are similar to those of [**G1A**]:[**4-C**] = 1:1, while the chemical shifts of **4-C** exhibit significant changes. These findings support that in the presence of excess amount of **4-C**, **G1A** remains involved in the H-bonding in the GC pair while cytidine undergoes some dynamic exchange. Similar trends were also observed for **G2A** when treated with excessive **4-C** (see Fig. S6 in the Supplementary data). DOSY NMR study on [**G2A**]:[**4-C**] and [**G2A**]:[**4-C**]$_2$ shows that the diffusion coefficients D_t of these two species are similar (see Fig. S7 in the Supplementary data), thus supporting that the stable GCC trimer species is unlikely, but it may be involved in a dynamic process.

Variable temperature NMR experiments were performed for [**G1A**]:[**4-C**]$_4$ to further probe the chemical-exchange process. As shown in Fig. 4, at temperatures below 208 K, one type of **G1A** and two types of **4-C** peaks (denoted as **4-C** and **4-C***) were observed. The sharp peaks between 10.5 and 13.4 ppm are assigned to N_2H (**G1A**), N_1H (**G1A**), and N_4H (**4-C**) of the GC pair. The broad resonance at 10.2 ppm can be assigned to a N_4H* of the non-bound **4-C***. Since the N_4H* proton remains broad and below 12 ppm, we can conclude that it does not belong to the typical [**4-C**]$_2$ dimer. Further lowering of the temperature to <188 K results in the

Fig. 1. Partial ^{1}H NMR spectra of (A) **4-C**, (B) **G1A**, and (C) [**G1A**]:[**4-C**] (CD_2Cl_2, 298 K).

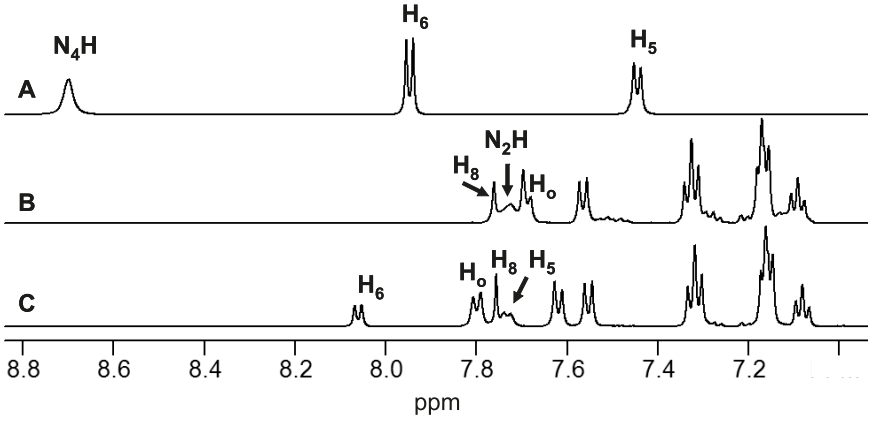

Fig. 2. Partial NOESY NMR spectrum of [**G1A**]:[**4-C**] (CD_2Cl_2, 228 K).

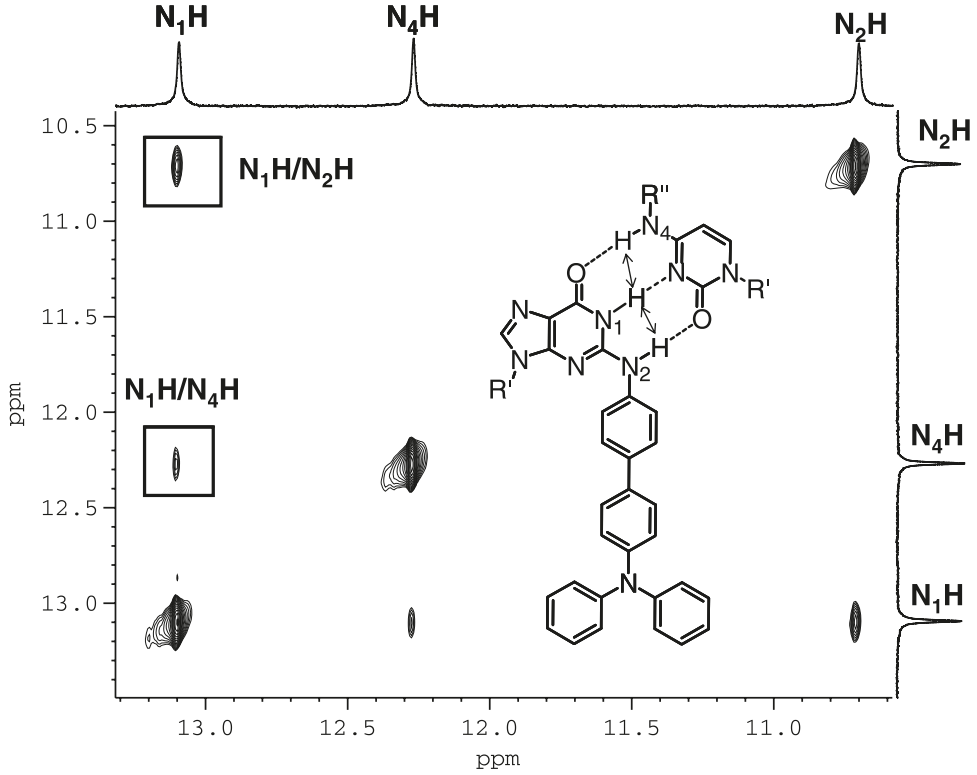

splitting of all non-exchangeable protons into **4-C** and **4-C*** as well.

To gain structural information about the dynamics of this system and to establish the connectivity between the GC pair and the non-bound **4-C***, COSY, NOESY, and ROESY NMR experiments were performed on the mixture of [**G1A**]:[**4-C**]$_2$ and [**G2A**]:[**4-C**]$_2$. The spectroscopic data for **G2A** are presented here because of the higher resolution and spectral quality compared with those for **G1A**. Complete spectral assignment for **G2A** and **4-C** resonances in [**G2A**]:[**4-C**]$_2$ was established using COSY. NOESY NMR was performed at 195 K, allowing the identification of closely related protons. Figure 5 shows the strong NOE signature cross peaks for [**G2A**]:[**4-C**]$_2$ between N_1H (**G2A**)/N_4H (**4-C**) protons indicative of Watson–Crick H-bonding. It is also worth noting that the NOE cross peaks observed between N_1H (**G2A**), N_4H (**4-C**), and N_4H* (**4-C***) with N_4Ac (**4-C**) and N_4Ac* (**4-C***) indicate that these protons are in close proximity to each other (see Fig. S8 in the Supplementary data). In the presence of excessive cytidine, all the cross peaks in the NOESY spectrum are of the same phase as the diagonal peaks.

To confirm NOE correlations and to distinguish them from chemical-exchange cross peaks, a 2D ROESY NMR spectrum was recorded at 195 K (Fig. 6), which reveals clear NOE cross peaks between the bound **4-C** and non-bound **4-C*** (e.g., N_4H (**4-C**)/N_4Ac* (**4-C***) and N_4H* (**4-C***)/N_4Ac (**4-C**)). In addition, the ribose protons associated with **4-C** in the [**G2A**]:[**4-C**] base pair are found to be in close proximity to H_6* (**4-C***) proton and vice versa. Furthermore, the H_6 proton (**4-C**) exhibits a NOE cross peak with the H_5* (**4-C***) proton. In addition, the chemical-exchange

Fig. 3. ^{1}H NMR spectral change of **G1A** with the addition of **4-C** (CD_2Cl_2, 298 K, [**G1A**] = 6.8×10^{-4} mol/L).

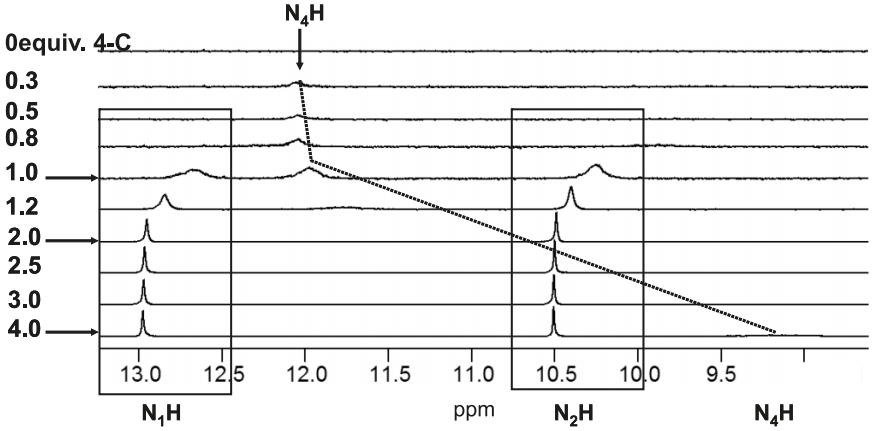

Fig. 4. Partial variable temperature NMR spectra of [**G1A**]:[**4-C**] = 1:4, (CD_2Cl_2, [**G1A**] = 6.8×10^{-4} mol/L).

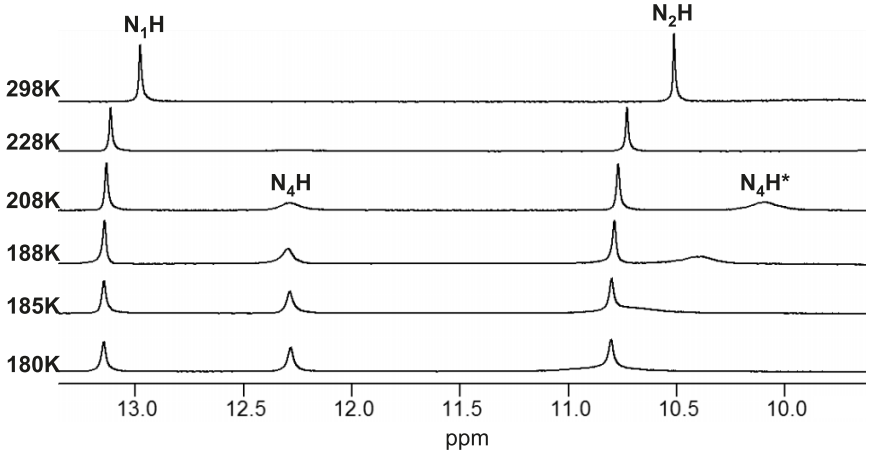

Fig. 5. Partial NOESY NMR spectrum of [**G2A**]:[**4-C**]$_2$ (CD_2Cl_2, 195 K).

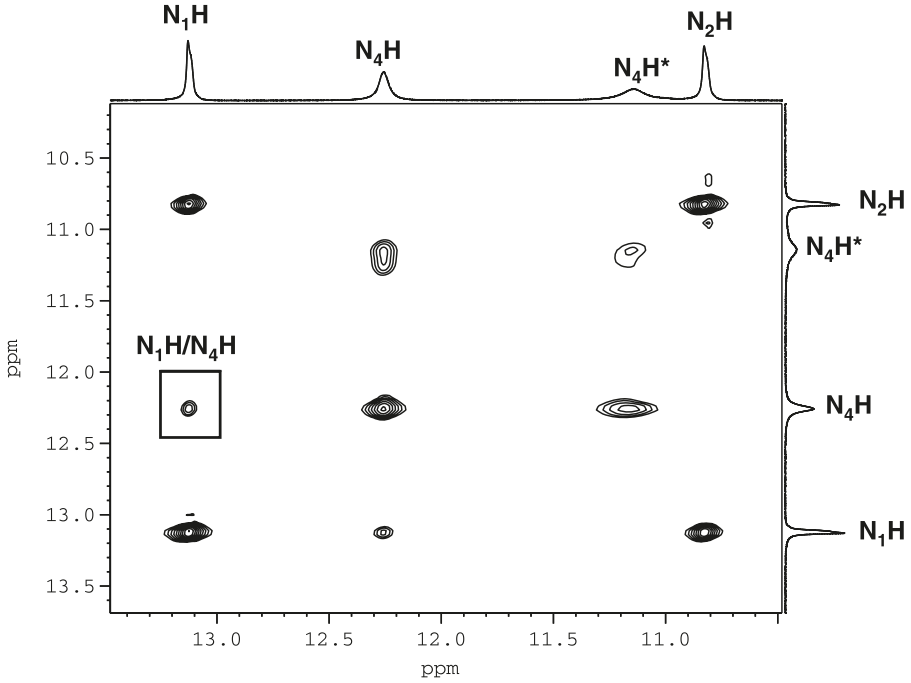

Fig. 6. Partial ROESY NMR spectra of [**G2A**]:[**4-C**]$_2$ (CD_2Cl_2, 195 K, red: NOE cross peaks, black: chemical-exchange cross peaks).

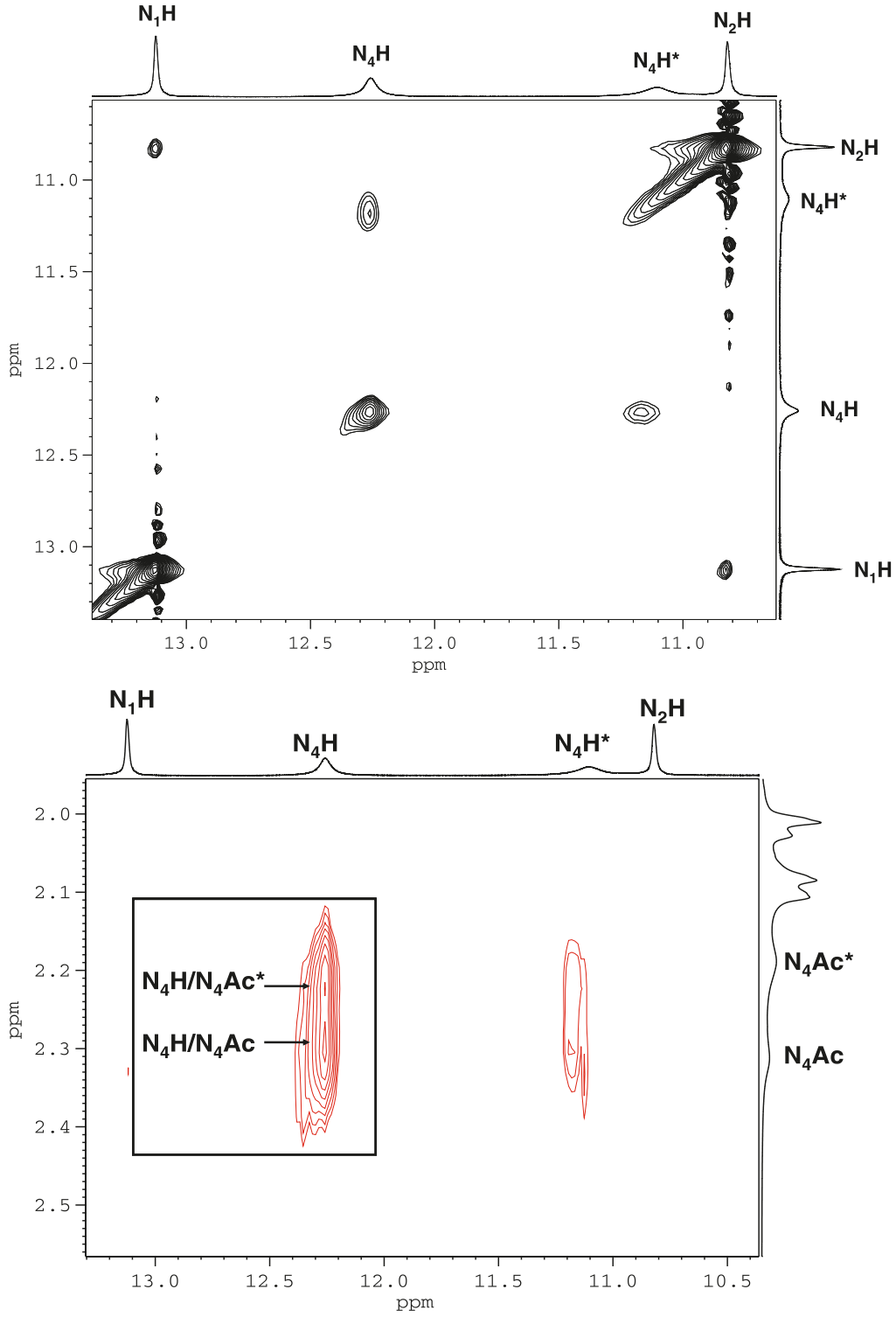

interaction was observed between the proton pairs of H_6 (**4-C**)/H_6* (**4-C***) and H_5 (**4-C**)/H_5* (**4-C***). The key protons that are involved in GC base pair formation all undergo chemical exchange with each other, which makes the complete assignment of the final structure difficult. However, on the basis of the relative chemical shifts of non-exchangeable protons and the specific NOE interactions shown in Fig. 6, it can be concluded that there are two types of cytidines, non-bound **4-C*** and bound **4-C** with **G2A**, which undergo chemical exchange with each other, leading to the averaging of the **4-C** signals at above 208 K. These findings are consistent with the presence of π–π stacking interactions between **4-C** in the [**G2A**]:[**4-C**] pair and non-bound **4-C***. Since **G2A** does not exhibit NOE with H_6* (**4-C***) and H_5* (**4-C***) protons the possibilities of π–π interactions between **G2A** in the [**G2A**]:[**4-C**] pair and **4-C*** can be ruled out.

Fig. 7. Fluorescence titrations of (A) **G1A** and (B) **G2A** with **4-C** (CH_2Cl_2, 2.5×10^{-5} mol/L, λ_{ex} = 362 nm (**G1A**) and 344 nm (**G2A**). Inset: Stern–Volmer plots at λ_{max}.

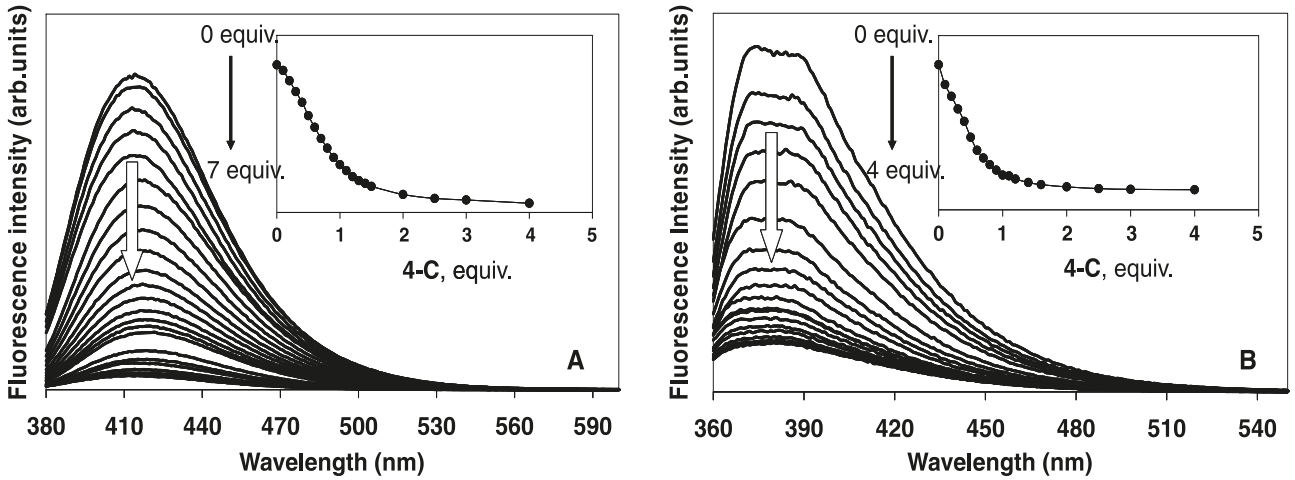

Fig. 8. Fluorescence spectra of **G1A** in the presence of A (left) or T (right) nucleosides with or without **4-C** (CH_2Cl_2).

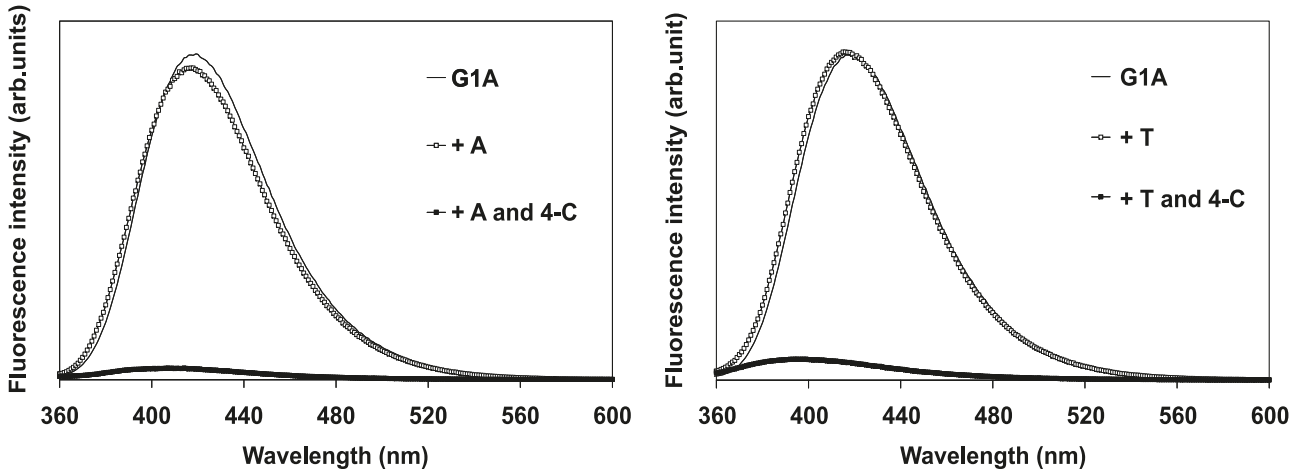

Using the variable temperature NMR data, the exchange rate k_c and the activation free energy $\Delta G^{\ddagger}$ for the exchange process were estimated to be 88 s^{-1} and 43 kJ mol^{-1}, respectively, at 208 K.

Fluorescence measurement

In contrast to the non-functionalized guanosines, which are weakly emissive in the UV region, **G1A** and **G2A** are highly emissive in the visible region, thus making it possible to monitor the G–C interactions by fluorescence spectroscopy as well. As shown in Fig. 7, the addition of **4-C** to the solution of **G1A** or **G2A** in CH_2Cl_2 results in quenching of the fluorescence emission of the N^2-arylguanosines. The Stern–Volmer plots support the formation of a stable 1:1 species with **4-C** (Fig. 6, inset), which is most likely responsible for the quenching of the guanosine emission. The binding constants for the GC pairs were determined to be 5×10^5 M^{-1} and 2×10^6 M^{-1} for **G1A** and **G2A**, respectively (see Fig. S9 in the Supplementary data).[9] These binding constants are in agreement with those reported in the literature for other GC pairs.[10]

As a control study, the fluorescence titration of **G2B** with **4-C** was also carried out (see Fig. S10 in the Supplementary data), which, not surprisingly, does not show any fluorescent quenching, thus further supporting the role of selective H-bonding between **G2A** and **4-C** in the fluorescence quenching. The selectivity of the fluorescence response of **G1A** and **G2A** toward cytidine was further confirmed by the competition experiments of 2′,3′,5′-*O*-triacetyladenosine (A) and 3′,5′-*O*-diacetylthymidine (T) with **4-C** for binding with **G1A** and **G2A**. As shown in Fig. 8, both A and T have no impact at all on the fluorescent spectrum of **G1A**. Similar results were also obtained for **G2A** (see Fig. S11 in the Supplementary data).

Molecular orbital calculations

Our previous TD-DFT calculations have established that the lowest electronic transitions and the fluorescence of **G1A** and **G2A** are π–π* transitions centered on guanine and the biphenyl-NAr_2 group.[4] To understand the origin of the fluorescence quenching upon GC pair formation, DFT calculations were performed for the [**G1A**]:[**4-C**] pair. The ground-state structure of the [**G1A**]:[**4-C**] pair was fully optimized at a B3-LYP/6–31G** level of theory and is presented in Fig. 9 along with the diagrams of the HOMO and LUMO levels.[11] The HOMO level of [**G1A**]:[**4-C**] consists

Fig. 9. HOMO and LUMO orbitals of the [**G1A**]:[**4-C**] base pair.

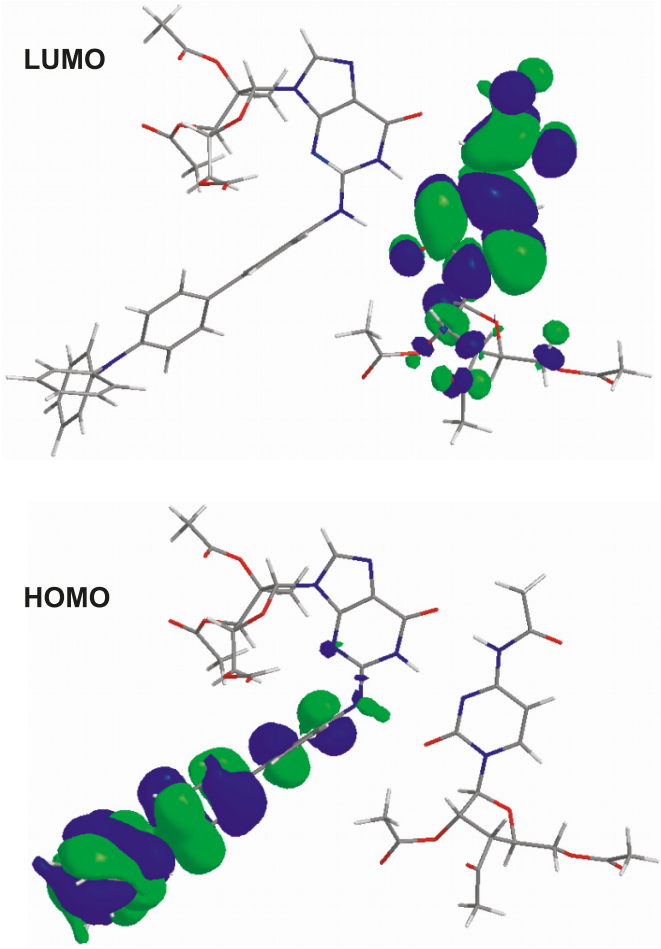

of π orbitals of the biphenyl-NPh_2 group while the LUMO level is made of entirely the π* orbitals of the cytosine ring. Hence, in contrast to **G1A**, where the lowest electronic transition is from a π–π* transition localized on the same part of the molecule, the lowest electronic transition of [**G1A**]:[**4-C**] is a charge transfer from the N^2 substituent to the cytosine ring. The low lying LUMO of the cytosine in the GC pair is therefore clearly responsible for quenching the emission of **G1A**. The guanine ring has no contributions to either the HOMO or the LUMO level of the GC pair, and probably acts as a bridge to facilitate H-bonds and electronic transitions between the N^2 substituent and the cytosine ring. Many examples of fluorescence quenching via intramolecular charge transfer in donor–acceptor types of GC base pair facilitated by H-bonding are known in the literature.[12] Our compounds are however the first example showing charge-transfer fluorescence quenching via the GC pair involving N^2-functionalized guanosines.

In summary, the aryl group at the N^2 site of guanosines **G1A** and **G2A** does not impede the selective formation of the H-bonding pair with cytidine. In fact, it facilitates the study of the G–C interactions via fluorescence spectroscopy owing to its highly fluorescent nature and the high sensitivity of the fluorescence spectrum toward G–C pair formation. An unusual exchange pathway between bound and free cytidine molecules and a potential π-stacked intermediate have been identified by NMR data.

Supplementary data

Supplementary data for this article are available on the journal Web site (canjchem.nrc.ca).

Acknowledgement

We thank the Natural Sciences and Engineering Research Council of Canada (NSERC) for financial support.

References

(1) (a) Alberti, P.; Bourdoncle, A.; Saccà, B.; Lacroix, L.; Mergny, J.-L. *Org. Biomol. Chem.* **2006**, *4* (18), 3383. doi:10.1039/b605739j. PMID:17036128.; (b) Sivakova, S.; Rowan, S. J. *Chem. Soc. Rev.* **2005**, *34* (1), 9. doi:10.1039/b304608g. PMID:15643486.; (c) Zhong, C.; Wang, J.; Wu, N.; Wu, G.; Zavalij, P. Y.; Shi, X. *Chem. Commun. (Camb.)* **2007**, (30): 3148. doi:10.1039/b704756h. PMID:17653370.; (d) Nikan, M.; Sherman, J. C. *J. Org. Chem.* **2009**, *74* (15), 5211. doi:10.1021/jo9001245. PMID:19518105.; (e) Kyogoku, Y.; Lord, R. C.; Rich, A. *Science* **1966**, *154* (748), 518. PMID:5916945.

(2) (a) Zakian, V. A. *Science* **1995**, *270* (5242), 1601. doi:10.1126/science.270.5242.1601. PMID:7502069.; (b) Guschlbauer, W.; Chanton, J. F.; Thiele, D. *J. Biomol. Struct.* **1990**, *8*, 91; (c) Parkinson, G. N.; Lee, M. P.; Neidle, S. *Nature* **2002**, *417* (6891), 876. doi:10.1038/nature755. PMID:12050675.

(3) (a) Liu, X. Y.; Kwan, I. C. M.; Wang, S.; Wu, G. *Org. Lett.* **2006**, *8* (17), 3685. doi:10.1021/ol061236w. PMID:16898792.; (b) Martić, S.; Liu, X. Y.; Wang, S.; Wu, G. *Chem. Eur. J.* **2008**, *14* (4), 1196. doi:10.1002/chem.200701411.

(4) Martić, S.; Wu, G.; Wang, S. *Inorg. Chem.* **2008**, *47* (18), 8315. doi:10.1021/ic800899b. PMID:18710219.

(5) (a) Harriman, A.; Magda, D. J.; Sessler, J. L. *J. Phys. Chem.* **1991**, *95* (4), 1530. doi:10.1021/j100157a005.; (b) Sessler, J. L.; Jayawickramarajah, J.; Gouloumis, A.; Pantos, G. D.; Torres, T.; Guldi, D. M. *Tetrahedron* **2006**, *62* (9), 2123. doi:10.1016/j.tet.2005.05.110.; (c) Sessler, J. L.; Jayawickramarajah, J.; Gouloumis, A.; Pantos, G. D.; Torres, T.; Guldi, D. M. *Chem. Soc. Rev.* **2007**, *36* (2), 314. doi:10.1039/b604119c. PMID:17264932.; (d) Sessler, J. L.; Sathiosatham, M.; Brown, C. T.; Rhodes, T. A.; Wiederrecht, G. *J. Am. Chem. Soc.* **2001**, *123* (16), 3655. doi:10.1021/ja005547s. PMID:11457097.; (e) Sessler, J. L.; Wang, B.; Harriman, A. *J. Am. Chem. Soc.* **1993**, *115* (22), 10418. doi:10.1021/ja00075a091.

(6) Kim, H. Y. H.; Cooper, M.; Nechev, L. V.; Harris, C. M.; Harris, T. M. *Chem. Res. Toxicol.* **2001**, *14* (9), 1306. doi:10.1021/tx010086p. PMID:11559047.

(7) Neidle, S.; Balasubramanian, S. *Quadruplex Nucleic Acids;* RCS Publishing: Cambridge, 2006.

(8) (a) Williams, L. D.; Chawla, B.; Shaw, B. R. *Biopolymers* **1987**, *26* (4), 591. doi:10.1002/bip.360260411.; (b) Williams, N. G.; Williams, L. D.; Shaw, B. R. *J. Am. Chem. Soc.* **1989**, *111* (18), 7205. doi:10.1021/ja00200a046.; (c) Williams, L. D.; Williams, N. G.; Shaw, B. R. *J. Am. Chem. Soc.* **1990**, *112* (2), 829. doi:10.1021/ja00158a050.

(9) (a) de la Peña, A. M.; Salinas, F.; Gómez, M. J.; Acedo, M. I.; Peña, M. S. *J. Inclusion Phenom. Mol. Recogn. Chem.*

1993, *15* (2), 131 doi:10.1007/BF00710222.; (b) Connors, K. A. *Binding Constants;* John Wiley & Sons: New York, 1987.

(10) (a) Encinas, S.; Simpson, N. R.; Andrews, M. D.; Ward, C. M.; White, C. M.; Armaroli, N.; Barigelletti, F.; Houlton, A. *N. J. Chem.* **2000**, *24* (12), 987. doi:10.1039/b006503j.; (b) Sessler, J. L.; Jayawickramarajah, J.; Gouloumis, A.; Torres, T.; Guldi, D. M.; Maldonado, S.; Stevenson, K. J. *Chem. Commun. (Camb.)* **2005**, (14): 1892. doi:10.1039/b418345b. PMID:15795778.; (c) Harriman, A.; Kubo, Y.; Sessler, J. L. *J. Am. Chem. Soc.* **1992**, *114* (1), 388. doi:10.1021/ja00027a074.

(11) Fisch, M. J.; Trucks, G. W.; Schlegel, H. B.; Scuseria, G. E.; Robb, M. A.; Cheesman, J. R., Jr.; Montgamery, J. A.; Vreven, T.; Kudin, K. N.; Burant, J. C.; Millam, J. M.; Iyengar, S. S.; Tomasi, J.; Barone, V.; Mennucci, B.; Cossi, M.; Scalmani, G.; Rega, N.; Petersson, G. A.; Nakatsuji, H.; Hada, M.; Ehra, M.; Toyota, K.; Fukuda, R.; Hasegawa, J.; Ishida, M.; Nakajima, T.; Honda, Y.; Kitao, O.; Nakai, H.; Li, M.; Klene, X.; Knox, J. E.; Hratchian, H. P.; Cross, J. B.; Bakken, V.; Adamo, C.; Jarmillo, J.; Gomperts, R.; Stratmann, R. E.; Yazyev, O.; Austin, A. J.; Cammi, R.; Pomelli, C.; Ochterski, J. W.; Ayala, P. Y.; Morokuma, K.; Voth, G. A.; Salvador, P.; Dannenberg, J. J.; Zakrzewski, V. G.; Dapprich, S.; Daniels, D.; Strain, M. C.; Farkas, O.; Malick, D. K.; Rabuck, A. D.; Raghavachari, K.; Foresman, J.; Ortiz, J. V.; Cui, Q.; Baboul, A. G.; Clifford, S.; Cioslowski, J.; Stefanov, B. B.; Liu, G.; Liashenko, A.; Piskorz, P.; Komaromi, I.; Martin, R. L.; Fox, D. J.; Keith, T.; Al-Laham, M. A.; Peng, C. Y.; Nanayakkara, A.; Challacombe, M.; Gill, P. M. W.; Johnson, B.; Chen, W.; Wong, M. W.; Bonzales, C.; Pople, J. A. *Gaussian 03, Revision C.02*; Gaussian Inc.: Wallingford, CT, 2004.

(12) (a) Mallajosyula, S. S.; Datta, A.; Pati, S. K. *Synth. Met.* **2005**, *155* (2), 398. doi:10.1016/j.synthmet.2005.09.022.; (b) Schwalb, N. K.; Temps, F. *J. Am. Chem. Soc.* **2007**, *129* (30), 9272. doi:10.1021/ja073448+. PMID:17622153.; (c) Ohshiro, T.; Umezawa, Y. *Proc. Natl. Acad. Sci. U.S.A.* **2006**, *103* (1), 10. doi:10.1073/pnas.0506130103. PMID: 16373509.